

First Hyperpolarizability of Polyaminoborane and Polyiminoborane Oligomers

Denis Jacquemin*

Laboratoire de Chimie Théorique Appliquée, Facultés Universitaires Notre-Dame de la Paix, rue de Bruxelles, 61, B-5000 Namur, Belgium

Received: July 1, 2004; In Final Form: August 16, 2004

The nonlinear optical properties of polyaminoborane, $-(\text{NH}_2-\text{BH}_2)_N-$, and polyiminoborane, $-(\text{NH}-\text{BH})_N-$, oligomers are studied by using ab initio schemes, taking explicitly into account the dynamic electron correlation effects. We report the evolution with chain length of the geometries, charges, dipole moments, polarizabilities, and first hyperpolarizabilities of both systems. The first hyperpolarizabilities are rationalized in terms of the delocalization/asymmetry interplay.

I. Introduction

In the search of large first hyperpolarizabilities (β), different strategies have been designed in order to obtain larger amplitudes than in inorganic crystals (LiNbO₃, KTP, etc.).¹ The most well known is the so-called push–pull strategy, in which a conjugated segment (polyene, phenyl groups, etc.) is capped at its ends by one electron-donor group on one side and one electron-acceptor group on the other.¹ These compounds, which possess both delocalizable electrons and large dipole moments present a first excited state corresponding to a charge transfer between the end moieties. As this first excited state is strongly coupled with the ground state, large β are obtained. To combine delocalizable electrons, which are necessary in order to reach large nonlinear optics (NLO) responses, and asymmetry (required because β is zero for centro-symmetric molecules), other schemes have been proposed. One of the most appealing is to take advantage of the presence of chiral atoms.² Once chirality is present, nonzero magnetic components to β are to appear. These mixed magnetic/electric components may be substantial in regard with the pure-electric components. On top of that, the chiral molecules present advantages for building macroscopic NLO systems. We refer the interested reader to the work of Persoons' group for more details (see, for instance, ref 3 and references therein). An alternative approach is to choose structures with large charge transfer, i.e., zwitterions,⁴ or to obtain a large charge separation by a distortion of the molecule.⁵ In the recent years, we have been interested in another alternative to push–pull molecules: the AB systems.^{6–12} In these systems, each unit is asymmetric (two different nuclei and two different bonds) and possess mobile electrons. Compared with other compounds, the AB chains present many advantages. Indeed, a purely electric response may be obtained for any chain length and the value of the polymer may be different from zero, which is not the case in push–pull chains.¹³ On top of that, these molecules may possess small dipole moments (i.e., small charge separation) but large β . Numerous AB compounds have been investigated.^{6–12} In regards to the evolution with chain length of β/N (N is the number of unit cells) of these systems, the compounds may be classified in three main categories: (i) β/N first increases and then saturates to the infinite chain limit, as

is the case for the polarizability (α/N) of an increasingly long compound. Polyphosphazene (PP) provides a typical example of this behavior.¹¹ In PP, the polymeric response is quite small, but by replacing the nitrogen of the backbone with silicon, one maintains the evolution but increases the polymeric response by 1 order of magnitude.¹¹ (ii) β/N increases for small chain lengths, reaches a maximum, and then decreases toward zero. This is the same behavior as in push–pull systems.¹⁴ Linear boron–nitrogen chains⁷ and all-trans polysilaacetylene [PSA, $-(\text{CH}=\text{SiH})_N-$]¹² belong to this second category. (iii) β/N is first negative, goes down, reaches a minimum, then increases, changes sign, and saturates toward the polymeric limit. This is typical of polyphosphinoborane (PPB)¹⁰ and all-trans polymethineimine (PMI) chains¹⁵ (at least at some level of theory). Qualitatively, these behaviors could be rationalized by splitting the total response in chain-end, and unit-cell components, both being affected by the asymmetry/delocalization interplay.^{6–12} In case (i), the chain-end component is either negligible or parallel to the unit cell component. In case (ii), the contribution of the unit cell is negligible with respect to the contribution of the chains end. This often means that the bond length alternation (Δr) found at the center of the AB chains tends to disappear as N increases. As the chain-end component becomes diluted in β/N , the polymeric ($N \rightarrow \infty$) response tends to zero. In case (iii), the chain-end and the unit-cell contributions to β have opposite signs, the former (latter) dominating the total response for short (long) oligomers.

In this paper, we investigate the polarizability and first hyperpolarizability of polyaminoborane (PAB) and polyiminoborane (PIB) (Figure 1), two inorganic polymers built with the alternation of boron and nitrogen. PAB has been synthesized by several groups since the 60's,^{16–24} whereas the synthesis of PIB is also described in the literature.^{25,26} To our knowledge, only one previous ab initio investigation has been performed for all-trans PAB and PIB.²⁷ The present study would flesh out our understanding of the relation between the delocalization/asymmetry interplay and the β of AB chains.

II. Computational Details

The calculations have been performed with the Gaussian03 program²⁸ by using the following procedure:

* E-mail: denis.jacquemin@fundp.ac.be. URL: <http://www.fundp.ac.be/jacquemd>. Research Associate of the Belgian National Fund for Scientific Research.

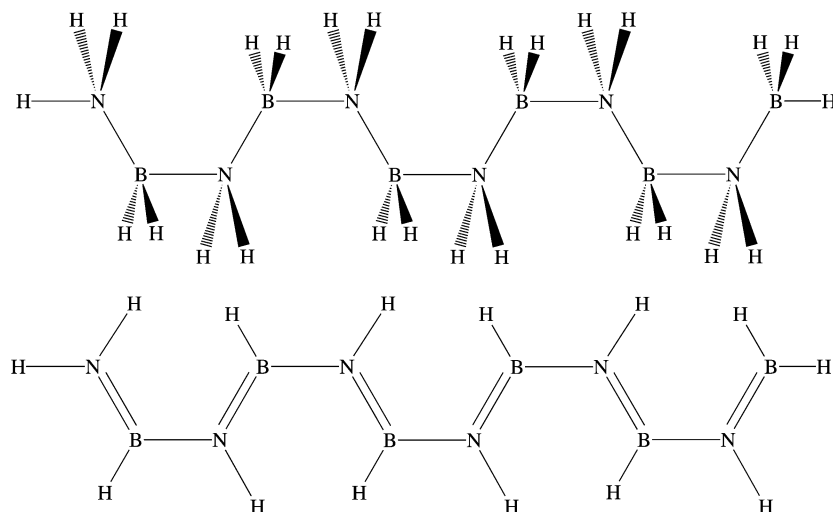


Figure 1. Schematic representation of trans-cisoid PAB (top) and PIB (bottom).

1. The ground state geometry of each oligomer has been determined by the optimization of its structural parameters. The only constraint was the use of the planar trans-cisoid (TC) conformation (Figure 1). Test calculations carried out at the MP2/6-311G(2d) level reveal that this conformation is the most stable planar structure for PAB, as it is the case for other AB systems, such as PP²⁹ or PPB.¹⁰ Other nonplanar conformers of PAB could exist,³⁰ but a study of these oligomers is beyond the scope of the present investigation. These optimizations have been performed within the one-parameter Perdew–Burke–Erzenrhof hybrid DFT functional³¹ (PBE0) and the second-order Møller–Plesset (MP2) levels of approximation using the 6-31G-(2d) and 6-311G(2d) basis sets, respectively. Indeed, these methods [PBE0/6-31G(2d) and MP2/6-311G(2d)] provide converged geometries that are close to the available experimental X-ray structures.^{30,32} After the geometry optimization, each oligomer has been oriented in the Cartesian frame so that the longitudinal axis runs through the center of the first and the last NB bonds.

2. In addition to the component of the dipole moment parallel to the longitudinal axis (μ_L), the partial atomic charges have been computed on the optimized geometries using the Mulliken, Merz–Kollman,³³ and CHELPG³⁴ schemes within the MP2/6-311G(2d) approximation.

3. Polarizabilities (α) and first hyperpolarizabilities (β) have been evaluated on the optimized geometries with two ab initio methods [HF/6-311G(2d) and MP2/6-311G(2d)]. PBE0 or other *conventional* DFT approaches cannot be used to compute the NLO properties of extended systems because they strongly overestimate the response of long oligomers.³⁵ In quasilinear chains, the longitudinal components of α and β tensors (α_L and β_L) often dominate the total response for sufficiently long chains. For example, the β_L of $N = 16$ of PIB (PAB) evaluated at the HF/6-311G(2d)/PBE0/6-31G(2d) level is 12 (5) times larger than the next larger component. For this reason, we focus on longitudinal components in this paper. Although they could make important contributions to the total static values in conjugated systems,^{36,37} the vibrational contributions to α and β (α^v and β^v) have been neglected because their practical determination at EC (electron correlated) levels remain difficult for extended oligomers. At the HF level, static α_L and β_L have been computed by using the coupled-perturbed Hartree–Fock (CPHF) method, whereas dynamic values have been obtained

with the time-dependent Hartree–Fock scheme (TDHF) method. The dynamic and static values are related by^{38,39}

$$\beta_L(-\omega_\sigma; \omega_1, \omega_2) = \beta_L(0; 0, 0)[1 + A\omega_L^2 + B\omega_L^4 + C\omega_L^6 + \dots] \quad (1)$$

$$\omega_L^2 = \omega_\sigma^2 + \omega_1^2 + \omega_2^2 \quad (2)$$

in which A and B are independent of the NLO process and the frequencies but depend on the molecules.^{40,41} At the MP2 level of approximation, static α_L and β_L have been evaluated by using the numerical finite-field procedure on the basis of the differentiation of the energies computed under several electric field amplitudes. We refer the reader to ref 7 for a complete description of this procedure. For the longer compounds investigated in this paper, it is not possible, in practice, to obtain dynamic NLO responses at the MP2 level. However, using the multiplicative correction,^{42,43} one can obtain reasonable estimates of these figures,⁴⁴ provided the static HF and MP2 values have the same sign (it is the case for PAB and PIB). In this paper, we adopt the usual sign convention for β_L , i.e., positive when orientated in the same direction as the dipole moment, negative otherwise.

4. The polymeric responses have been obtained by extrapolating the oligomeric values. To carry out the extrapolations, we define the β_L (and μ_L and α_L) per unit cell as $\Delta\beta_L(N) = (1/2)[\beta_L(N) - \beta_L(N-2)]$. This definition removes most of the chain-end effects and leads to a fast convergence toward the asymptotic limit ($N \rightarrow \infty$). Our fitting procedure allows us to obtain the average $\Delta\beta_L(\infty)$ and its standard deviation. We refer the reader to ref 15 for more details.

III. Results

A. Geometries. It is well known that the bond length alternation (Δr) has a crucial impact on the NLO properties of conjugated molecules.⁴⁵ Tables 1 and 2 give the Δr obtained at the center of PAB and PIB. For PAB, an experimental X-ray structure of substituted dimers is available.³² It turns out that the central bond is shorter (1.576 Å) than the terminal bonds (1.595 and 1.599 Å). Being negative, our PBE0/6-31G(2d) and MP2/6-311G(2d) Δr reproduce this feature. Using our convention,⁴⁶ the experimental Δr is -0.02 Å, whereas the MP2/6-311G(2d) and PBE0/6-31G(2d) Δr are -0.04 Å. This difference

TABLE 1: Bond Length Alternation (Å), Charge Alternation (e), Longitudinal Dipole Moment, Static Polarizability, and Static First Hyperpolarizability (au) of Trans-Cisoid PAB Chains^a

<i>N</i>	Δr	Δq^b	Δq^c	Δq^d	μ_L [HF]	μ_L [MP2]	α_L [HF]	α_L [MP2]	β_L [HF]	β_L [MP2]
X/6-311G(2d)/MP2/6-311G(2d)										
2	-0.042	1.17	0.36	0.52	-1.65	-1.62	52	55	-24	-48
4	-0.019	1.27	-0.58	-0.12	-3.78	-3.72	108	116	-149	-214
6	-0.003	1.27	-0.55	-0.21	-6.13	-6.04	167	180	-294	-401
8	0.004	1.28	-0.75	-0.28	-8.58	-8.46	226	246	-440	-584
X/6-311G(2d)/PBE0/6-31G(2d)										
2	-0.035	1.16	0.31	0.50	-1.59	-1.57	53	56	-24	-48
4	-0.020	1.26	-0.57	-0.14	-3.67	-3.61	108	116	-149	-216
6	-0.004	1.26	-0.58	-0.19	-5.98	-5.90	167	181	-295	-406
8	0.003	1.27	-0.73	-0.31	-8.38	-8.28	226	246	-442	-591
10	0.008	1.27	-0.73	-0.35	-10.83	-10.70	286	312	-589	-772
12	0.011	1.27	-0.76	-0.32	-13.30	-13.15	346	378	-734	-950
14	0.013				-15.77	-15.61	407	444	-879	-1126
16	0.014				-18.26	-18.08	466	510	-1024	-1302
∞^e	0.016				-1.26	-1.25	30	33	-72	-86
Δ_∞^e	0.002				0.02	0.02	1	1	1	2

^a All results have been obtained with the 6-311G(2d) basis set on the PBE0/6-31G(2d) and MP2/6-311G(2d) geometries. Δq have been obtained with the MP2 approach. At the bottom of the table, the extrapolated polymeric values are given (see the text for more details on the procedure used to obtain these values). 1 au of $\mu = 2.5418$ D. 1 au of $\alpha = 1.6488 \cdot 10^{-41} \text{ C}^2 \text{ m}^2 \text{ J}^{-1} = 0.14818 \text{ \AA}^3$. 1 au of $\beta = 3.2063 \cdot 10^{-53} \text{ C}^3 \text{ m}^3 \text{ J}^{-2} = 8.641 \cdot 10^{-33} \text{ esu}$. ^b Calculated on the basis of Mulliken charges. ^c Calculated on the basis of MK charges. ^d Calculated on the basis of CHELPG charges. ^e ∞ gives the extrapolated value where Δ_∞ is the estimated extrapolation error, i.e. polymeric values are given by $\infty \pm \Delta_\infty$.

TABLE 2: Bond Length Alternation (Å), Charge Alternation (e), Longitudinal Dipole Moment, Static Polarizability, and Static First Hyperpolarizability (au) of Trans-Cisoid PIB Chains (See Table 1 for More Details).

<i>N</i>	Δr	Δq^a	Δq^b	Δq^c	μ_L [HF]	μ_L [MP2]	α_L [HF]	α_L [MP2]	β_L [HF]	β_L [MP2]
X/6-311G(2d)/MP2/6-311G(2d)										
2	0.064	0.93	1.20	1.53	-0.38	-0.49	48	53	36	50
4	0.026	0.88	1.60	1.83	-0.00	-0.08	104	122	(-) ^d 129	(-) ^d 197
6	0.014	0.89	1.57	1.84	0.51	0.50	165	198	403	660
8	0.008	0.89	1.57	1.85	1.07	1.14	227	276	726	1229
X/6-311G(2d)/PBE0/6-31G(2d)										
2	0.060	0.92	1.33	1.52	-0.38	-0.48	48	53	37	52
4	0.024	0.87	1.60	1.84	0.02	-0.06	104	121	127	(-) ^d 192
6	0.013	0.88	1.56	1.83	0.55	0.54	165	197	401	654
8	0.008	0.88	1.55	1.84	1.14	1.20	227	275	724	1220
10	0.005	0.88	1.57	1.84	1.74	1.89	290	355	1073	1842
12	0.003	0.87	1.61	1.83	2.35	2.60	354	436	1434	2491
14	0.002				2.97	3.31	417	516	1801	3154
16	0.001				3.59	4.03	481	597	2174	3829
∞^e	-0.003				0.32	0.37	32	41	191	349
Δ_∞^e	0.003				0.01	0.01	1	1	5	11

^a Calculated on the basis of Mulliken charges. ^b Calculated on the basis of MK charges. ^c Calculated on the basis of CHELPG charges. ^d β_L is negative because it points towards the direction opposite to the dipole moment. However, the direction of β_L is constant for all oligomers and β_L could be considered positive for all chain lengths: it is parallel to the dipole moment of the polymer. ^e ∞ gives the extrapolated value where Δ_∞ is the estimated extrapolation error; i.e. polymeric values are given by $\infty \pm \Delta_\infty$.

is probably related to the presence in the experimental compound of side groups which could tune the geometry and the conformation of PAB. This negative Δr means that short PAB oligomers favor a cis-transoid over a trans-cisoid conformation. For long chains, the Δr becomes positive, consistently with a trans-cisoid conformation. The MP2/6-311G(2d) Δr obtained for PAB and PIB are small; for $N = 8$, they are 0.004, 0.008, 0.024,²⁹ 0.014,¹⁰ and 0.070 Å,⁴⁷ for PAB, PIB, PP, PPB, and PA, respectively. In PAB, the Δr converges quickly with chain length and the polymeric Δr is predicted to be small, but nonzero [PBE0/6-31G(2d) = 0.016 ± 0.002 Å]. This contrasts with the saturated carbon system, i.e., polyethylene, in which all bond lengths are equal. The PIB Δr seems to converge to a small negative, but nonzero value, which is consistent with the nonzero $\Delta\mu_L(\infty)$ of PIB. Indeed, the polymeric Δr is predicted to be -0.003 ± 0.003 Å [PBE0/6-31G(2d)]. This negative (or null) Δr means that very long PIB would favor a cis-transoid over a trans-cisoid conformation. In contrast to PA (PE), PIB (PAB) presents almost equal (different) bond lengths. Therefore, the

consequence of the dehydrogenation of PAB is a decrease of the magnitude (and probably sign reversal for very long chains) of Δr . Interestingly, for PAB, calculations in the all-trans conformation reveal a zero Δr .²⁷ This nonalternating all-trans/alternating trans-cisoid pattern has already been noticed in PPB chains.⁴⁸

From a more methodological point of view, we see that the MP2/6-311G(2d) and PBE0/6-31G(2d) Δr exactly follow the same trends with respect to chain length. In addition, except for the smallest chain, PBE0 and MP2 provide similar Δr (within $\sim 1-2 \times 10^{-3}$ Å) for both PAB and PIB so PBE0 geometries can be trusted for longer chains.

B. Charges and Dipole Moments. While Δr describes the bond length alternation, other parameters are important for assessing the delocalization and the asymmetry along the oligomeric backbone. Among these parameters is the nuclear alternation, i.e., the chemical nature of A and B in AB systems. As a crude approximation to this parameter, we use the difference between the charges on adjacent atoms, i.e., the

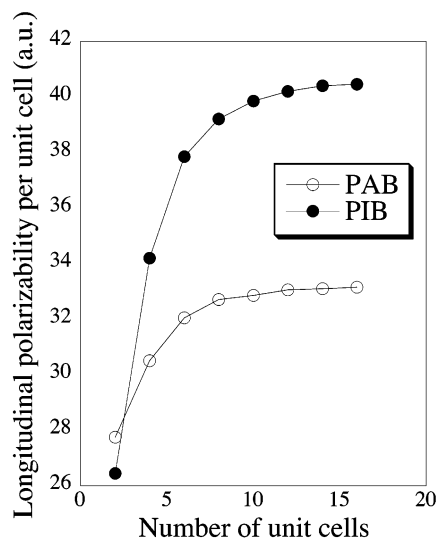


Figure 2. Evolution with chain length of the MP2/6-31G(2d)/PBE0/6-31G(2d) longitudinal polarizability per unit cell, $\Delta\alpha_L(N)$, of PAB and PIB.

charge alternation $\Delta q = q^B - q^N$ measured at the center of the chain. Within the Mulliken approximation, Δq converges extremely fast with respect to N and becomes almost constant if $N \geq 4$ ($\Delta q = 1.3$ e and 0.9 e, for PAB and PIB, respectively). However, Mulliken charges are not always reliable, and MK or CHELPG schemes often provide charges in better agreement with experimental data.⁴⁹ The saturation speed is slower with MK or CHELPG charges, but for long oligomers, they predict the charge separation of PAB to be -0.8 e and -0.3 e. This $\Delta q^{\text{MK}} = -0.8$ e in PAB is probably related to the TC conformation as Δq^{MK} is positive for other conformations;³⁰ it is smaller than in PP where the P and N atoms almost exchange one electron (i.e., $\Delta q^{\text{MK}} \approx 2$ e)²⁹ and is similar to PPB for which we obtained $\Delta q^{\text{MK}} = 0.91$ e.¹⁰ The effect of reduction is described very differently by Mulliken and MK/CHELPG schemes. In the former, the charge transfer is decreased by 30% in PIB. In the two latter, removing the hydrogen atoms changes the sign and strongly increases the magnitude of Δq . In ref 10, a similar disagreement between the impact of the reduction on the Mulliken and MK charges has been found.

Tables 1 and 2 give the μ_L of PAB and PIB, respectively. The $\Delta\mu_L$ evolution with chain length of both systems presents a standard shape: it increases (in magnitude) for small oligomers then enters the saturation regime where it converges toward the polymeric value. At the MP2/6-31G(2d) level, the dehydrogenation changes the sign and strongly decreases the magnitude of $\Delta\mu_L(\infty)$ from 3.18 to 0.94 D. These values may be compared to the 4.35 D $\Delta\mu_L(\infty)$ for PP⁵⁰ or to the 5.59 D for PPB.¹⁰ As a first approximation, μ_L primarily depends on the asymmetry,⁵¹ so the evolution of $\Delta\mu_L(\infty)$ when going from PAB to PIB could be related to a change of sign and smaller asymmetry in PIB. As PIB μ_L actually reverses sign between $N = 4$ and $N = 6$, this is also consistent with the smaller values of Δr and $\Delta q^{\text{Mulliken}}$ in PIB.

C. (Hyper)polarizabilities. 1. Static Values. Tables 1 and 2 give the static α_L and β_L for PAB and PIB, whereas Figures 2 and 3 depict the evolution with chain length of the static $\Delta\alpha_L$ and $\Delta\beta_L$. For both systems, the PBE0 and MP2 geometries lead to very similar responses, so that we can directly trust the lower-level geometries. Indeed, the largest difference is 1 au (2%) for α_L , whereas for β_L , it is 9 au (4%).

As expected for increasingly long compounds,^{51–55} the $\Delta\alpha_L$ of PAB (and PIB) increases rapidly with chain length for short

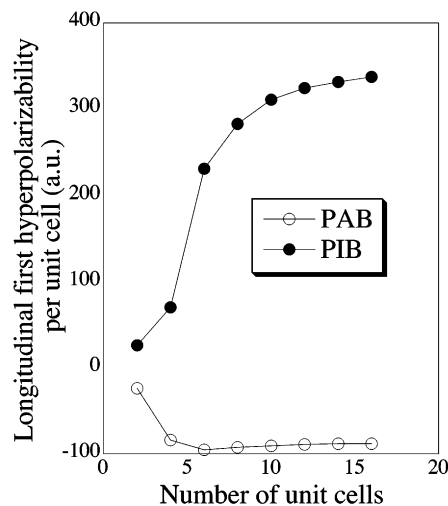


Figure 3. Evolution with chain length of the MP2/6-31G(2d)/PBE0/6-31G(2d) longitudinal first hyperpolarizability per unit cell, $\Delta\beta_L(N)$, of PAB and PIB.

oligomers then enters the saturation regime where it tends toward the asymptotic value characterizing the infinite polymer. This polymeric value per unit cell is 33 au (41 au) for PAB (PIB). For comparison, PA⁵⁶ and polysilane⁵⁷ present $\Delta\alpha_L(\infty)$ that are close to 131 au, whereas for the phosphorus equivalent of PAB and PIB, PPB and dehydrogenated PPB (DHPPB), we obtained ϕ 67 au and 178 au, respectively.¹⁰ As α does not depend on the asymmetry but only on the delocalizability, this emphasizes that PIB chains are slightly more delocalizable than PAB, although both are poorly polarizable. The polarizability enhancement due to hydrogen removal is related to an increase of electron mobility, which in turn can be associated with the smaller Δr and $\Delta q^{\text{Mulliken}}$ of PIB. To further rationalize these findings, natural bond order⁵⁸ (NBO) analysis has been performed on both systems. For long oligomers, chain-end perturbations are reduced and the NBO analysis predicts for PAB a localized structure constituted of single bonds only (occupancy > 1.98 e) in PAB, corresponding to a $sp^{2.0}$ ($sp^{3.5}$) character of the nitrogen (boron) atoms. For PIB, the NBO analysis shows an alternance of single (occupancy > 1.95 e) and double bonds (occupancy > 1.95 e and 1.79 e), with $sp^{1.5}$ ($sp^{2.1}$) hybrid character for nitrogen (boron) atoms. The remaining binding electrons in the double bonds present an almost 100% p character on both atoms. In other words, the NBO yields figures that are quite consistent with a sp^3/sp^2 representation when going from PAB to PIB (at least for boron), which in turn is consistent with the observed delocalizability increase. However, the single/double alternance in PIB seems questionable in regards to the small computed Δr . This diversity of these results is not a surprise if one compares to PP²⁹ or DHPPB¹⁰ cases where the nature of the bonds is also differently predicted by several analyses.

In PAB, $\Delta\beta_L$ is always negative. Its magnitude first increases, reaches a maximum for $N = 6$, and then saturates downward a slightly smaller polymeric limit. This shape remains for the different selected levels of theory and is similar to that found for cis-transoid PSA.¹² To rationalize this shape, one can divide β into different components (see Introduction). Indeed, the total β value can be split into chain-end (NH_3 versus BH_3 terminal groups) and unit cell contributions. Additionally, the unit cell contribution can itself be divided into nuclear alternation (N versus B) and bond alternation (longer versus shorter bonds). In the case of PAB, the evolution of $\Delta\beta_L$ can be interpreted as follows: (i) for short oligomers, the chain-end contribution

TABLE 3: Dynamic Longitudinal Polarizability and First Hyperpolarizability (au) of trans-Cisoid PAB and PIB Chains (All Results Have Been Obtained with the TDHF/6-311G(2d)//PBE0/6-31G(2d) Method. See Table 1 for Mode Details).

<i>N</i>	static		$\lambda = 1907$ nm			$\lambda = 1064$ nm		
	$\alpha_L(0; 0)$	$\beta_L(0; 0, 0)$	$\alpha_L(-\omega; \omega)$	$\beta_L(-\omega; \omega, 0)$	$\beta_L(-2\omega; \omega, \omega)$	$\alpha_L(-\omega; \omega)$	$\beta_L(-\omega; \omega, 0)$	$\beta_L(-2\omega; \omega, \omega)$
PAB								
2	53	-24	53	-24	-24	53	-24	-25
4	108	-149	100	-150	-152	109	-152	-158
6	167	-295	167	-297	-301	168	-301	-314
8	226	-442	227	-445	-451	228	-451	-470
10	286	-589	287	-592	-600	288	-601	-627
12	346	-734	347	-739	-748	349	-749	-722
14	407	-879	407	-885	-897	409	-898	-937
16	466	-1024	468	-1031	-1044	470	-1046	-1091
PIB								
2	48	37	48	37	38	48	38	42
4	104	127	105	128	130	105	130	136
6	165	401	165	404	412	167	413	441
8	227	724	228	732	748	230	750	804
10	290	1073	291	1084	1109	294	1111	1195
12	354	1434	355	1450	1483	358	1487	1602
14	417	1801	419	1822	1865	423	1869	2017
16	481	2174	483	2199	2250	487	2256	2436

(which is negative) dominates the total response, (ii) due to the increase of electron delocalization, the amplitude of chain-end contribution increases when the chain lengthens, (iii) for long chains, the unit-cell contribution (which is negative but smaller) dominates the β response, and (iv) for very long oligomers $\Delta\beta_L$ is constant, each unit cell accounting for the same contribution to β_L . Similarly to cis-transoid PSA chains, the combination of (i), (ii), (iii), and (iv) explains the presence of an extremum before the saturation zone (see ref 12 and references therein). Since the delocalization is limited in PAB, the saturation of β_L toward the polymeric limit is fast and the polymeric value, $\Delta\beta_L(\infty)$, is quite small (-86 au at the MP2/6-311G(2d)//PBE0/6-31G(2d) level).

As could be expected from the important variations of Δr , Δq , and $\Delta\mu_L$, the amplitude and shape of the $\Delta\beta_L$ versus N curve is deeply modified when shifting from PAB to PIB. Indeed, in PIB, the shape of the curve (Figure 3) does not present a sign change nor a minimum and is similar to a "polarizability" curve: an increase due to the delocalization followed by the saturation toward the polymeric limit. This monotonic evolution indicates that the chain-end contribution to β_L is probably small and parallel to the unit-cell contribution. Also, the polymeric $\Delta\beta_L$ (349 au at the MP2/6-311G(2d)//PBE0/6-31G(2d) level) is larger than in PAB. This can be related to the larger delocalizability in PIB ($\Delta\alpha_L$ is larger than in PAB while Δr is smaller). PIB $\Delta\alpha_L(\infty)$ is only 24% larger than in PAB, whereas for $\Delta\beta_L(\infty)$, the percentage is 305%, showing that the differences are much stronger for nonlinear effects than for linear responses. Note that PIB is also more symmetric, see $\Delta\mu_L$, than PAB. This could, in theory, lead to a falloff of β_L and means that the β_L of PAB is limited by the delocalization rather than by the asymmetry factor. This is consistent with the model calculations performed on AB polymers⁵⁹ which have shown that bond and charge alternations have to be small in order to obtain large macromolecular β_L , i.e., it seems preferable to have small asymmetry ($\Delta\mu_L$) and large delocalization ($\Delta\alpha_L$) rather than the reverse.

2. *Dynamic Values.* In the sum-over-states framework,⁶⁰ the (hyper)polarizabilities are proportional to the inverse of the energy differences between the ground and excited states. In a crude approximation, this means that large NLO would be obtained for small-gap systems. As the frequency dispersion effects tend to be larger for small-gap compounds, one can conclude that the larger the static β , the larger the frequency

dispersion effects. This simple qualitative approach is verified for PAB and PIB, for which dynamic β values are given in Table 3 (two standard LASER frequencies have been used). For the longest chain treated ($N = 16$), $\beta(-2\omega; \omega, \omega)$ is increased by 2% (7%) in the case of PAB for $\lambda = 1907$ nm (1064 nm). The increase is almost two times larger in PIB: 3% (12%) for $\lambda = 1907$ nm (1064 nm). These percentages are relatively small because, with the LASER frequencies used, resonance is still far away due to the large gaps of PAB and PIB. For the longer PAB and PIB chains, the dynamic/static ratio is almost constant (with respect to N), so that these percentages should be almost constant for the polymer. As ω_L^2 [see eqs 1 and 2] is similar for $\beta(-2\omega; \omega, \omega)$ when $\lambda = 1907$ nm and for $\beta(-\omega; \omega, 0)$ when $\lambda = 1064$ nm, these two processes lead to almost identical β , as confirmed by Table 3.

Dispersion plots obtained for the dodecamer of PAB and PIB are shown in Figure 4. We have obtained the A (eq 1) value for the dodecamer of PAB and PIB by a least-squares fitting with the function $[1 + A\omega_L^2 + B\omega_L^4 + C\omega_L^6]$ on a set of $\beta(-\omega; \omega, 0)$ points corresponding to frequencies = 0.000; 0.005; ..., 0.060 au. It turns out that $A = 5$ for PAB and $A = 9$ for PIB, confirming that frequency dispersion effects are larger in the

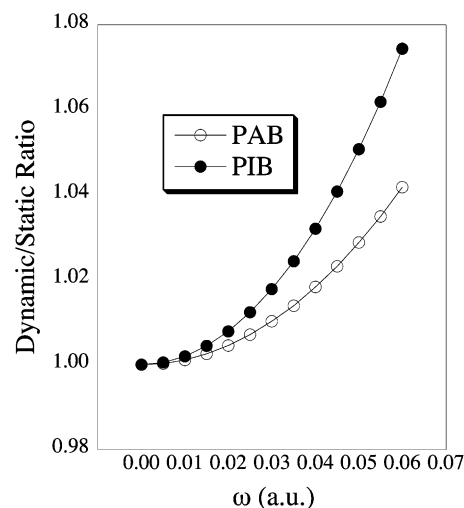


Figure 4. TDHF/6-311G(2d)//PBE0/6-31G(2d) dispersion curve (optical rectification) obtained for the dodecamer of PAB and PIB. The values reported are the ratio with respect to the static response: $\beta_L(-\omega; \omega, 0)/\beta_L(0; 0, 0)$.

latter system. For comparison, the A value for α,ω -nitro,amino-transhexatriene is 45,⁴⁴ whereas the dodecamer of PPB and DHPPB present A of 6 and 30, respectively.¹⁰

IV. Conclusion

We have investigated the geometry, charges, dipole moments, polarizability, and first hyperpolarizability of polyaminoborane and polyiminoborane. It appears that both systems present a limited delocalizability (small polarizability). PAB has a substantial asymmetry (large dipole moment). The bond alternation of PIB is very small compared to other polymers (polyphosphazene, polyacetylene, etc.). Therefore, going from PAB to PIB, an increase of electron mobility and a decrease of asymmetry is noted. As a consequence, the static $\Delta\beta_L(\infty)$ of PAB is multiplied by 5 when the hydrogen atoms are removed. This factor becomes larger when frequency dispersion effects are taken care of. Compared to the corresponding phosphorus polymers (PPB and DHPPB), PAB and PIB show smaller polarizabilities and first hyperpolarizabilities.¹⁰ This is probably related to the "softer" character of phosphorus with respect to nitrogen.

The static $|\beta_L|/W$ (first hyperpolarizability per unit of weight) of the systems here investigated can easily be estimated from the corresponding $|\Delta\beta_L(\infty)|$: $0.01 \times 10^{-30} \text{ cm}^5 \text{ esu}^{-1} \text{ g}^{-1} \text{ mol}$ for PAB and $0.03 \times 10^{-30} \text{ cm}^5 \text{ esu}^{-1} \text{ g}^{-1} \text{ mol}$ for PIB. One may compare these values with the $0.02 \times 10^{-30} \text{ cm}^5 \text{ esu}^{-1} \text{ g}^{-1} \text{ mol}$ reported for PPB,¹⁰ $0.10 \times 10^{-30} \text{ cm}^5 \text{ esu}^{-1} \text{ g}^{-1} \text{ mol}$ for the 3-methyl-4-nitroaniline (MNA) monomer,⁶¹ $0.06 \times 10^{-30} \text{ cm}^5 \text{ esu}^{-1} \text{ g}^{-1} \text{ mol}$ for N -(4-nitrophenyl)- L -prolinol (NPP),⁶² $0.66 \text{ cm}^5 \text{ esu}^{-1} \text{ g}^{-1} \text{ mol}$ for α,ω -nitro,amino-transhexatriene,⁴⁴ and $4.2 \times 10^{-30} \text{ cm}^5 \text{ esu}^{-1} \text{ g}^{-1} \text{ mol}$ for PMI.⁶ At this point, one can finally conclude that both PAB and PIB probably present a weak potential for NLO applications.

Acknowledgment. D.J. thanks the Belgian National Fund for his research associate position. D.J. thanks (in alphabetical order): Prof. J.-M. André (FUNDP, Namur) for his perpetual support, Dr. C. Lambert (FUNDP, Namur) for giving us the opportunity to perform high-memory calculations and Dr. E. A. Perpète (FUNDP, Namur) for countless fruitful discussions. Most calculations have been performed on the Interuniversity Scientific Computing Facility (ISCF), installed at the Facultés Universitaires Notre-Dame de la Paix (Namur, Belgium), for which the authors gratefully acknowledge the financial support of the FNRS-FRFC and the "Loterie Nationale" for the convention number 2.4578.02 and of the FUNDP.

References and Notes

- (1) Kanis, D. R.; Ratner, M. A.; Marks, T. J. *Chem. Rev.* **1994**, *94*, 195–242.
- (2) Verbiest, T.; Van Elshocht, S.; Kauranen, M.; Hellemans, C.; Snauwaert, J.; Nuckolls, C.; Katz, T. J.; Persoons, A. *Science* **1998**, *282*, 913–915.
- (3) Verbiest, T.; Sioncke, S.; Persoons, A.; Vylicky, L.; Katz, T. J. *Angew. Chem., Int. Ed.* **2002**, *41*, 3882–3884.
- (4) Sitha, S.; Rao, J. L.; Bhanuprakash, K.; Choudary, B. M. *J. Am. Chem. Soc.* **2001**, *105*, 8727–8733.
- (5) Keinan, S.; Zojer, E.; Brédas, J. L.; Ratner, M. A.; Marks, T. J. *J. Mol. Struct. (THEOCHEM)* **2003**, *633*, 227–235.
- (6) Jacquemin, D.; Champagne, B.; André, J. M. *Chem. Phys. Lett.* **1998**, *284*, 24–30.
- (7) Jacquemin, D.; Perpète, E. A.; Champagne, B. *Phys. Chem. Chem. Phys.* **2002**, *4*, 432–440.
- (8) Jacquemin, D.; Perpète, E. A.; Champagne, B.; André, J. M.; Kirtman, B. *Recent Research Developments in Physical Chemistry*; Transworld Research Network: Trivandrum, India, 2002; Vol. 6.
- (9) Jacquemin, D.; Champagne, B.; André, J. M. *Macromolecules* **2003**, *36*, 3980–3985.
- (10) Jacquemin, D. *J. Phys. Chem. A* **2004**, *108*, 500–506.
- (11) Jacquemin, D.; Quinet, O.; Champagne, B.; André, J. M. *J. Chem. Phys.* **2004**, *120*, 9401–9409.
- (12) Jacquemin, D.; Perpète, E. A.; André, J. M. *J. Chem. Phys.* **2004**, *120*, 10317–10327.
- (13) Morley, J. O.; Docherty, V. J.; Pugh, D. *J. Chem. Soc., Perkin Trans. 2* **1987**, 1351–1355.
- (14) Jacquemin, D.; Champagne, B.; Perpète, E. A.; Luis, J.; Kirtman, B. *J. Phys. Chem. A* **2001**, *105*, 9748–9755.
- (15) Champagne, B.; Jacquemin, D.; André, J. M.; Kirtman, B. *J. Phys. Chem. A* **1997**, *101*, 3158–3165.
- (16) Brown, M. P.; Heseltine, R. W. *J. Inorg. Nucl. Chem.* **1967**, *29*, 1197–1201.
- (17) Kwon, C. T. J.; McGee, H. A. *Inorg. Chem.* **1970**, *9*, 2458–2461.
- (18) Denton, D. L.; Johnson, A. D.; Hickam, C. W., Jr.; Bunting, R. K.; Shore, S. G. *J. Inorg. Nucl. Chem.* **1975**, 1037–1038.
- (19) Pustcioglu, S. Y.; McGee, H. A., Jr.; Fricke, A. L.; Hassler, J. C. *J. Appl. Polym. Sci.* **1977**, *21*, 1561–1567.
- (20) Komm, R.; Geanangel, R. A.; Liepins, R. *Inorg. Chem.* **1983**, *22*, 1684–1686.
- (21) Geanangel, R. A.; Rabalais, J. W. *Inorg. Chim. Acta* **1985**, *97*, 59–64.
- (22) Kim, D. P.; Moon, K. T.; Kho, J. G.; Economy, J.; Gervais, C.; Babonneau, F. *Polym. Adv. Technol.* **1999**, *10*, 702–712.
- (23) Baitalow, F.; Baumann, J.; Wolf, G.; Jaenicke-Rössler, K.; Leitner, G. *Thermochim. Acta* **2002**, *391*, 159–168.
- (24) Gervais, C.; Babonneau, F. *J. Organomet. Chem.* **2002**, *657*, 75–82.
- (25) Paetzold, P.; von Bennigsen-Mackiewicz, T. *Chem. Ber.* **1981**, *114*, 298–305.
- (26) Paetzold, P. *Adv. Inorg. Chem.* **1987**, *31*, 123–170.
- (27) Abdurahman, A.; Albrecht, M.; Shukla, A.; Dolg, M. *J. Chem. Phys.* **1999**, *110*, 8819–8824.
- (28) Frisch, M. J.; Trucks, G. W.; Schlegel, H. B.; Scuseria, G. E.; Robb, M. A.; Cheeseman, J. R.; Montgomery, J. A., Jr.; Vreven, T.; Kudin, K. N.; Burant, J. C.; Millam, J. M.; Iyengar, S. S.; Tomasi, J.; Barone, V.; Mennucci, B.; Cossi, M.; Scalmani, G.; Rega, N.; Petersson, G. A.; Nakatsuji, H.; Hada, M.; Ehara, M.; Toyota, K.; Fukuda, R.; Hasegawa, J.; Ishida, M.; Nakajima, T.; Honda, Y.; Kitao, O.; Nakai, H.; Klene, M.; Li, X.; Knox, J. E.; Hratchian, H. P.; Cross, J. B.; Adamo, C.; Jaramillo, J.; Gomperts, R.; Stratmann, R. E.; Yazyev, O.; Austin, A. J.; Cammi, R.; Pomelli, C.; Ochterski, J. W.; Ayala, P. Y.; Morokuma, K.; Voth, G. A.; Salvador, P.; Dannenberg, J. J.; Zakrzewski, V. G.; Dapprich, S.; Daniels, A. D.; Strain, M. C.; Farkas, O.; Malick, D. K.; Rabuck, A. D.; Raghavachari, K.; Foresman, J. B.; Ortiz, J. V.; Cui, Q.; Baboul, A. G.; Clifford, S.; Cioslowski, J.; Stefanov, B. B.; Liu, G.; Liashenko, A.; Piskorz, P.; Komaromi, I.; Martin, R. L.; Fox, D. J.; Keith, T.; Al-Laham, M. A.; Peng, C. Y.; Nanayakkara, A.; Challacombe, M.; Gill, P. M. W.; Johnson, B.; Chen, W.; Wong, M. W.; Gonzalez, C.; Pople, J. A. *Gaussian 03*, revision B.04; Gaussian, Inc.: Pittsburgh, PA, 2003.
- (29) Sun, H. *J. Am. Chem. Soc.* **1997**, *119*, 3611–3618.
- (30) E. A. Perpète, personal communication.
- (31) Adamo, C.; Barone, V. *J. Chem. Phys.* **1999**, *110*, 6158–6170.
- (32) Jaska, C. A.; Temple, K.; Lough, A. J.; Manners, I. *J. Am. Chem. Soc.* **2003**, *125*, 9424–9434.
- (33) Besler, B. H.; Merz, K. M.; Kollman, P. A. *J. Comput. Chem.* **1990**, *11*, 431–439.
- (34) Breneman, C. M.; Wiberg, K. B. *J. Comput. Chem.* **1990**, *11*, 361–373.
- (35) Champagne, B.; Perpète, E.; Jacquemin, D.; van Gisbergen, S.; Baerends, E.; Soubra-Ghaoui, C.; Robins, K.; Kirtman, B. *J. Phys. Chem. A* **2000**, *104*, 4755–4763.
- (36) Champagne, B.; Kirtman, B. *Chem. Phys.* **1999**, *245*, 213–226.
- (37) Kirtman, B.; Champagne, B.; Bishop, D. M. *J. Am. Chem. Soc.* **2000**, *122*, 8007–8012.
- (38) Bishop, D. M.; De Kee, D. W. *J. Chem. Phys.* **1996**, *104*, 9876–9887.
- (39) Bishop, D. M.; De Kee, D. W. *J. Chem. Phys.* **1996**, *105*, 8247–8249.
- (40) Hättig, C. *Mol. Phys.* **1998**, *94*, 455–460.
- (41) Bishop, D. M. *Mol. Phys.* **1998**, *94*, 989–989.
- (42) Sekino, H.; Bartlett, R. J. *Chem. Phys. Lett.* **1995**, *234*, 87–93.
- (43) Aiga, F.; Itoh, R. *Chem. Phys. Lett.* **1996**, *251*, 372–380.
- (44) Jacquemin, D.; Champagne, B.; Hättig, C. *Chem. Phys. Lett.* **2000**, *319*, 327–334.
- (45) Meyers, F.; Marder, S. R.; Pierce, B. M.; Brédas, J. L. *J. Am. Chem. Soc.* **1994**, *116*, 10703–10714.
- (46) Δr is computed as the difference between the length of the central B–N bond and the length of the previous bond. For the PAB dimer ($N = 2$), $\Delta r = d_{\text{B(H}_2\text{)-N(H}_2\text{)}} - d_{\text{B(H}_2\text{)-N(H}_2\text{)}}$.

- (47) Perpète, E. A.; Champagne, B. *J. Mol. Struct. (THEOCHEM)* **1999**, 487, 39–45.
- (48) Jacquemin, D.; Lambert, C.; Perpète, E. A. *Macromolecules* **2004**, 37, 1009–1015.
- (49) Sigfridsson, E.; Ryde, U. *J. Comput. Chem.* **1998**, 19, 377–395.
- (50) From MP2/6-31G(d)/MP2/6-31G(d) calculations performed on the TC conformers of PP.
- (51) Jacquemin, D.; Champagne, B.; Kirtman, B. *J. Chem. Phys.* **1997**, 107, 5076–5087.
- (52) Hurst, G. J. B.; Dupuis, M.; Clementi, E. *J. Chem. Phys.* **1988**, 89, 385–395.
- (53) Kirtman, B. *Chem. Phys. Lett.* **1988**, 143, 81–83.
- (54) Champagne, B.; Mosley, D. H.; André, J. M. *J. Chem. Phys.* **1994**, 100, 2034–2043.
- (55) Toto, J. L.; Toto, T. T.; de Melo, C. P.; Kirtman, B.; Robins, K. A. *J. Chem. Phys.* **1996**, 104, 8586–8592.
- (56) Toto, T. T.; Toto, J. L.; de Melo, C. P.; Hasan, M.; Kirtman, B. *Chem. Phys. Lett.* **1995**, 244, 59–64.
- (57) Kirtman, B.; Hasan, M. *J. Chem. Phys.* **1992**, 96, 470.
- (58) Reed, A. E.; Curtiss, L. A.; Weinhold, F. *Chem. Rev.* **1988**, 88, 899–926.
- (59) Champagne, B.; Jacquemin, D.; André, J. M. *SPIE Proc.* **1995**, 2527, 71–81.
- (60) Orr, B. J.; Ward, J. F. *Mol. Phys.* **1971**, 20, 513–526.
- (61) Castet, F.; Champagne, B. *J. Phys. Chem. A* **2001**, 105, 1366–1370.
- (62) Champagne, B.; Perpète, E. A.; Legrand, T.; Jacquemin, D.; André, J. M. *J. Chem. Soc., Faraday Trans.* **1998**, 94, 1547–1553.